Impact of deconditioning on the secondary electron yield of Cu surfaces in particle accelerators

V. Petit,[1,2] M. Taborelli,[1] D. A. Zanin,[1] H. Neupert,[1] P. Chiggiato,[1] and M. Belhaj[2]

[1]*European Organization for Nuclear Research, CERN, 1211, Geneva 23, Switzerland*
[2]*ONERA The French Aerospace Lab, 31055 Toulouse, France*

(Received 6 July 2020; accepted 6 August 2020; published 8 September 2020)

Electron cloud is a critical phenomenon in particle accelerators operating with high intensity and positively charged beams, as it is responsible for beam instabilities, vacuum degradation, and heat load on cryogenic sections. Electron clouds provoke a conditioning of the beam pipe that is reflected on the reduction of its secondary electron yield (SEY). However, such a benefit is partially lost when vacuum sectors are vented for maintenance of accelerators; this phenomenon is called deconditioning. Samples removed from accelerators are also vented before surface analysis. Deconditioning amplifies the electron cloud at the resuming of beam operation and, on the other hand, hinders the understanding of the electron multipacting mechanism from surface analysis data. In this paper, copper deconditioning was studied for samples stored in a desiccator over months. Immediately after air exposure, an increase of the SEY is observed. This increase is driven by carbon recontamination and copper hydroxide growth on the conditioned surface as observed by x-ray photoelectron spectroscopy. After deconditioning, the differences of SEY present on the tested samples partially vanish, in particular, for surfaces conditioned to a maximum SEY below 1.45, limiting the level of accessible information when analyzing components extracted from accelerators. However, for a maximum SEY above 1.45, the differences remain visible for at least 8 weeks of storage. Among different storage conditions, vacuum efficiently stops the SEY increase over time. Besides, the memory effect of the conditioning is preserved over at least 4 months when closing the vacuum system on itself after venting with a clean and dry gas.

DOI: 10.1103/PhysRevAccelBeams.23.093101

I. INTRODUCTION

The electron cloud effect, i.e., the exponential multiplication of electrons in the beam vacuum, is a critical phenomenon for particle accelerators operating with high-intensity positively charged beams [1–4]. Several techniques aiming at hindering the occurrence of the cloud, e.g., by reducing the secondary electron yield (SEY) of the beam pipe surface, have thus been developed over the years: low SEY thin film coatings [5,6], laser engineered surfaces [7,8], and introduction of a solenoid field [9] and of clearing electrodes [10]. However, for several materials used in the beam vacuum system, the bombardment of the beam pipe surface by the electrons results in a spontaneous decrease of the cloud intensity, eventually down to a level compatible with beam operation [11–13]. This so-called conditioning effect has been demonstrated to result from the reduction of the SEY of the surface during electron irradiation [14,15].

Several surface modifications are observed during low-energy electron irradiation, which are responsible for the corresponding SEY decrease. In the case of copper, the material of the beam-pipe surface in the cryogenic arcs of the LHC at CERN, surface cleaning by electron stimulated desorption (ESD) was reported [16,17], leading to the decomposition of copper hydroxide $Cu(OH)_2$ and part of the adsorbed hydrocarbons [18–20]. In addition, carbon graphitization of the airborne carbon layer was observed [14,19–22].

When an electron-irradiated surface is exposed to air, the reverse process—namely, deconditioning—occurs, leading to a partial erasing of the conditioning state. A loss of the conditioning state is a concern for the operation of particle accelerators, since it translates into a reactivation of the electron cloud when resuming beam operation, after technical stops including maintenance and venting. In addition, for diagnostic studies, it excludes the access to the original *in situ* conditioning state of the surface as induced by the electron cloud, unless an *in situ* surface characterization setup [15,23–26] or the possibility to transfer components to the laboratory under vacuum [15] exists. Unfortunately, in complex devices such as cryogenic superconducting magnets as those in the LHC arcs, such

in situ analyses or sample transfer are not available. Extracting vacuum components to analyze their surface is therefore possible only after venting the corresponding parts [27]. Understanding the mechanisms and kinetics of the deconditioning would thus enable one to define a strategy to preserve as much as possible the conditioning state of electron-irradiated components extracted for analysis or vented for machine maintenance. In addition, such a study is required to define the limits of accessible information when performing analyses on such components.

In this work, several aspects of the deconditioning process of copper are investigated, such as its kinetics and its impact on the SEY and on differences of SEY which are possibly present *in situ* between different parts of the accelerator before venting. The deconditioning mechanisms are studied by monitoring the surface chemistry evolution by x-ray photoelectron spectroscopy (XPS) over storage time in a desiccator, which provides a reasonably reproducible atmosphere. Then, the impact of the storage atmosphere on the deconditioning is investigated and reported.

II. EXPERIMENTAL

A. Experimental setup

The experiments were carried out at room temperature in a baked UHV system composed of two main chambers linked through a transfer line. The first chamber (base pressure 5×10^{-9} mbar) is equipped for XPS analysis at 45° emission with a nonmonochromatic Mg Kα source ($h\nu = 1253.6$ eV). The energy scale is calibrated using the Cu $2p_{3/2}$ (932.7 eV) and the Au $4f_{7/2}$ (84.0 eV) lines. The second chamber (base pressure 5×10^{-10} mbar) hosts a SEY measuring setup and an electron flood gun enabling sample irradiation for conditioning. The samples are inserted in the system through the XPS chamber load lock.

B. SEY measurement

The SEY δ is defined as the ratio of the total number of emitted electrons I_{sec} to the number of impinging electrons I_p. SEY measurements were carried out at normal incidence, between 30 and 1730 eV of electron landing energy, at steps of 50 eV. The setup is similar to the one described in Ref. [28] and consists of an electron gun, a collector biased at +40 V, and the sample itself, biased at −15 V. When primary electrons impinge on the sample surface, the latter emits secondary electrons which are accelerated to the positively biased collector. During the measurement, the sample-to-ground I_{sa} and collector-to-ground I_{sec} currents are simultaneously acquired. In this configuration,

$$I_p = I_{\mathrm{sec}} + I_{\mathrm{sa}}.$$

The SEY is thus computed:

$$\delta = \frac{I_{\mathrm{sec}}}{I_{\mathrm{sec}} + I_{\mathrm{sa}}}.$$

The primary beam is deflected to the collector between the acquisition of each point of the SEY curve to limit the irradiation dose and sample conditioning during the SEY measurement (estimated corresponding dose for one complete SEY measurement: 2×10^{-7} C/mm^2). The maximum SEY scattering (standard deviation) observed over three locations of a sample, including the error due to the current measurement and nonuniformity of the sample, is typically 0.02.

C. Sample preparation and conditioning

This study was carried out on 15×20 mm^2 oxygen-free electronic grade (OFE) copper samples. All samples were wet-chemically cleaned in a commercial detergent, following the procedure for the chemical cleaning of UHV parts at CERN [29]. The sample state after such cleaning procedure and approximately 2–3 months of storage in aluminum foil and polyethylene bag in air is referred to as "as received." On such samples, the presence of copper hydroxide on top of a Cu_2O layer is deduced by XPS from the presence of components at 934.4 and 932.6 eV, respectively, on the Cu 2p line [30]. Silicon up to a maximum amount of 1.5 at.% is also found on the surface, resulting from the presence of silicates in the cleaning detergent.

Conditioning was carried out using a flood gun irradiating the sample at normal incidence and with 250 eV electrons. The sample current during irradiation was about 15 μA, as measured with a sample bias of +15 V. The area irradiated by the flood gun at the sample position was evaluated to 133 mm^2 using a Faraday cup. Partially conditioned samples were obtained by stopping the conditioning before reaching a dose of 10^{-2} C/mm^2, where the SEY decrease is found to saturate [19,20]. The flood gun was extensively degassed during the night prior the experiment.

After the suitable level of conditioning and acquisition of the XPS spectrum, the samples were transferred back to the load lock, vented with nitrogen, and immediately brought into the chosen storage conditions.

D. Storage conditions

To investigate the influence of the storage conditions on the deconditioning kinetics, fully conditioned samples (conditioned to 10^{-2} C/mm^2) were stored in different controlled atmospheres: (i) unbaked vacuum (base pressure 10^{-8} mbar) after 1 h transfer in air, (ii) saturated vapor pressure of water at room temperature, (iii) closed stainless-steel tube previously cleaned with the CERN standard procedure for UHV parts, at atmospheric pressure of air, and (iv) desiccator (closed glass container hosting silica gel, humidity level below 10%). In the desiccator, the samples were wrapped in aluminum foil to allow stacking.

For the last three cases, the transfer time from the UHV analysis system to the storage container was below 2 min.

All storage environments were selected either because they represent extreme situations of humidity in air (saturated vapor pressure of water) or conditions under which samples extracted from an accelerator could be stored before analysis. Furthermore, the dry air of a desiccator is similar to the gas used for the venting of the LHC arcs (ultrapure nitrogen and oxygen mixture). At defined times, the samples were extracted from storage to be analyzed and immediately placed back in the storage container after analysis.

III. RESULTS

A. Deconditioning kinetics

To evaluate the rate of the deconditioning occurring on an electron-irradiated surface exposed to dry air, the evolution of the maximum SEY δ_{max} of two fully conditioned twin samples (A and B) was followed during storage in a desiccator. The corresponding plot is shown in Fig. 1. For storage times shorter than 2 weeks, the trend is identical for the two samples. The maximum SEY follows a logarithmic increase. The SEY increase occurring in the first minutes of air exposure is equivalent to the one occurring in the next 2 weeks of storage. However, after 4 months of storage, the SEY of both samples is still significantly lower than the one for the as received state. This demonstrates that the memory effect of conditioning persists after 4 months of storage in a desiccator.

The SEY curves of sample B in its as received and fully conditioned states as well as for different storage durations are shown in Fig. 2. In agreement with a previous study [18], the energy of the maximum SEY E_{max} shifts to higher values during conditioning. A shift back toward the initial energy immediately starts at air exposure and is fully completed, within the resolution of the measurements, after only 8 h of storage. A similar behavior was observed for sample A.

B. Evolution of surface chemistry

The decrease of copper hydroxide and carbon signals, as well as carbon graphitization, were identified as main characteristics of an electron-irradiated copper surface [18]. The reverse processes are expected to occur when this surface is exposed to air. The evolution of the surface chemistry was followed for sample B, previously presented in Figs. 1 and 2. The XPS Cu 2p line of the as received and conditioned states of the surface, together with its evolution during storage, are shown in Fig. 3(a). As expected, the $Cu(OH)_2$ component at 934.4 eV [30] and the corresponding Cu(II) satellite between 939 and 949 eV [30] disappear after full conditioning. A clear increase of this component and of the satellite intensity are observed over storage time in a desiccator. After 4 months of storage, these components remain still lower than before any conditioning. This behavior is coherently observed in the O 1s line [Fig. 3(b)]: during storage, an increase of the component at 531.3 eV corresponding to hydroxide [31] is observed. In parallel, an increase of carbon coverage was observed during storage, due to airborne contamination. Figure 4 shows the evolution of the maximum SEY, the atomic carbon surface concentration, and the ratio of the intensity of the Cu $2p_{3/2}$ line at 934.4 eV to that at 932.6 eV, corresponding to $I_{Cu(OH)_2}/I_{Cu,Cu_2O}$, for the same sample. The time $t = 0$ corresponds to the fully conditioned state, just before venting.

Both the carbon concentration and the hydroxide amounts are observed to increase during storage. Since both adsorbed hydrocarbons and copper hydroxide increase the SEY of clean surfaces [28,32,33], their buildup on the

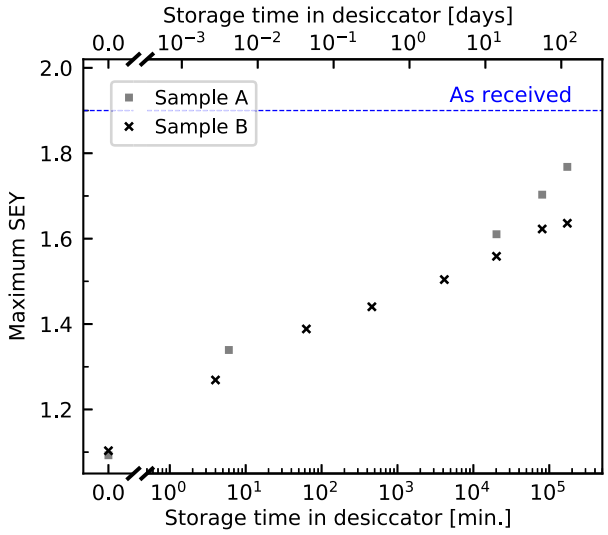

FIG. 1. Evolution of the maximum SEY of two fully conditioned OFE copper samples (A and B) during storage in a desiccator. The time $t = 0$ represents the fully conditioned state.

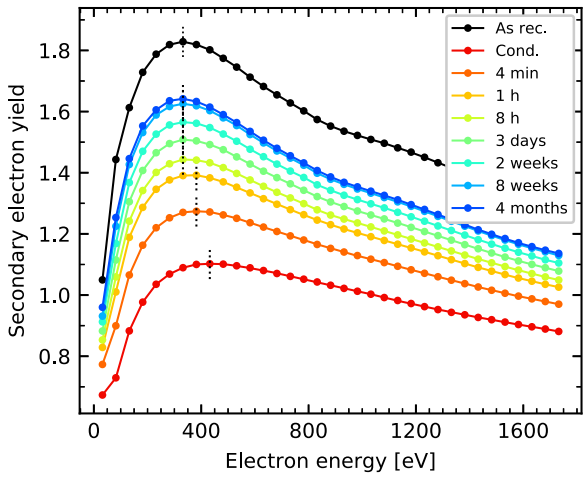

FIG. 2. SEY curves of an OFE copper sample stored in a desiccator after full conditioning. The dotted lines indicate the energy position of the maximum SEY.

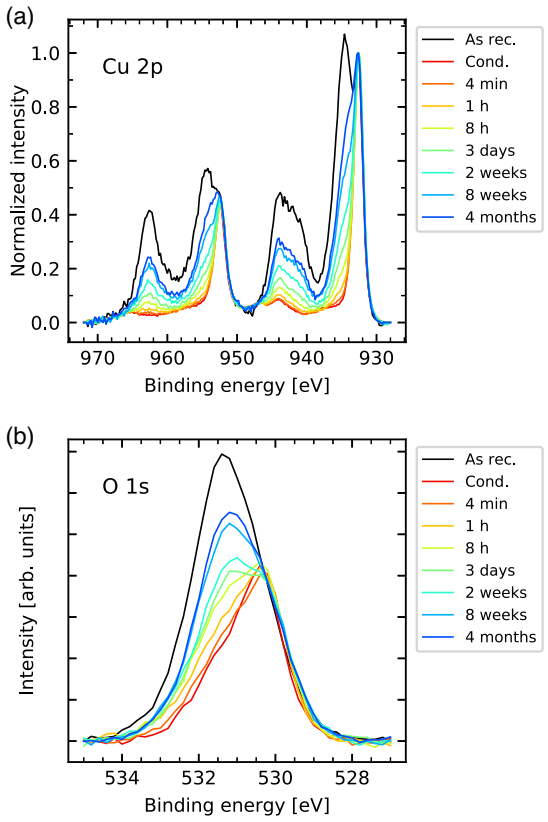

FIG. 3. X-ray photoelectron spectra of an OFE copper sample in the as received and fully conditioned states and after different storage times in a desiccator: (a) Cu 2p lines (normalization to the intensity at 932.6 eV after linear background subtraction) and (b) corresponding O 1s lines, after Shirley background subtraction.

conditioned surface contributes to its deconditioning. However, the growth kinetics is different for the two species. Indeed, immediately after venting, the carbon content significantly increases, while copper hydroxide is not yet detected on the surface. For storage times below 4 minutes, the SEY increase is therefore driven by carbon recontamination. For storage times between 4 minutes and 8 hours, both the carbon amount and hydroxide contributions increase. For times longer than 8 hours, the carbon uptake seems to have saturated for this storage condition and reaches in this case the as received surface content. The further SEY increase seems therefore driven only by hydroxide buildup.

The airborne origin of the carbon recontamination is also visible through the evolution of the C 1s line shape, shown in Fig. 5. During conditioning, the C 1s line shifts from 284.8 to 284.4 eV, translating a graphitization of the adventitious carbon layer [34], and the carboxyl group contribution at 288.5 eV disappears, as already observed [18–20]. During storage, the C 1s line shifts back toward its initial position, as expected for a recontamination by hydrocarbons (sp^3 hybridization). In addition, carboxyl

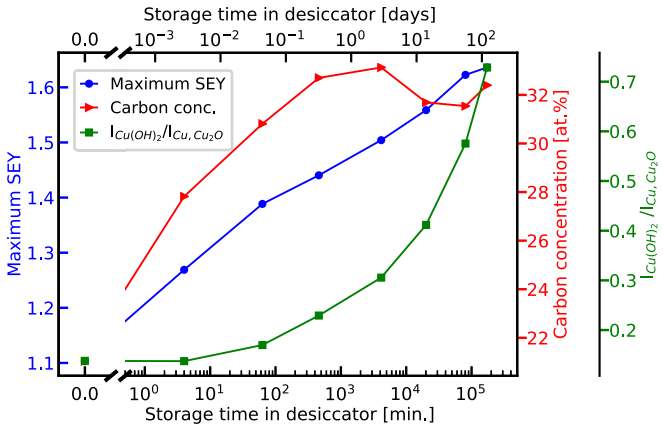

FIG. 4. Evolution of the maximum SEY, atomic surface concentration of carbon and ratio $I_{Cu(OH)_2}/I_{Cu,Cu_2O}$ over storage time in a desiccator after full conditioning. The time $t = 0$ corresponds to the fully conditioned state, just before venting, and the three data points for the maximum SEY, carbon concentration, and $I_{Cu(OH)_2}/I_{Cu,Cu_2O}$ overlap there.

groups are readsorbed on the surface as witnessed by the increase of the intensity at 288.5 eV. After 4 months in the desiccator, the maximum of the C 1s line is only at 0.1 eV away from its initial (as received) position; i.e., the shift back is mostly completed and the remaining difference with respect to the as received state is within the energy accuracy of the experimental setup. This shift back results from a globally less graphitic carbon overlayer due to the readsorption of sp^3 carbon. A conversion of the graphitic film into sp^3 carbon is unlikely [35,36]. The same trends were observed for sample A, for the hydroxide and carbon recontamination.

C. Impact of deconditioning on the SEY contrasts

To evaluate the impact of deconditioning on the attenuation of the SEY contrasts, i.e., the differences of SEY which are possibly present *in situ* between different parts of

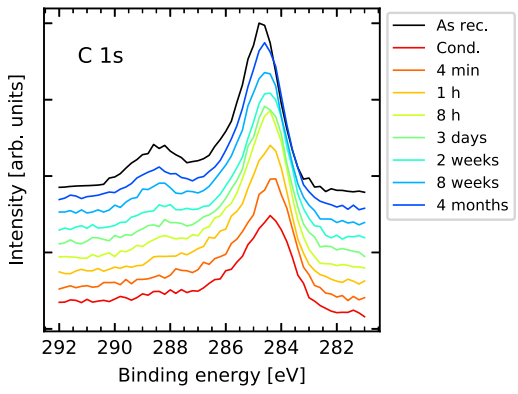

FIG. 5. C 1s lines of an OFE copper sample in its as received and conditioned states and after different storage times in a desiccator.

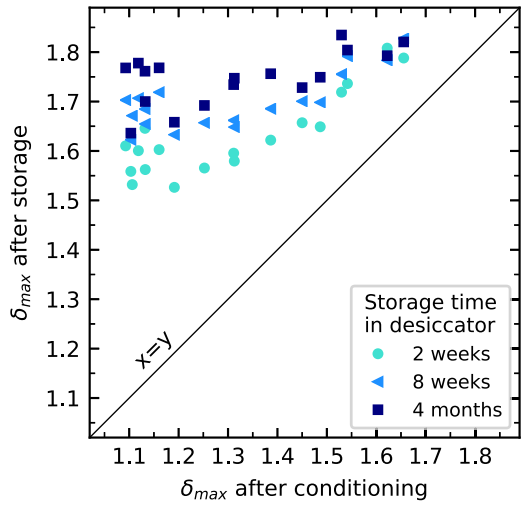

FIG. 6. Evolution of the maximum SEY during storage in a desiccator of OFE copper samples conditioned to different maximum SEY.

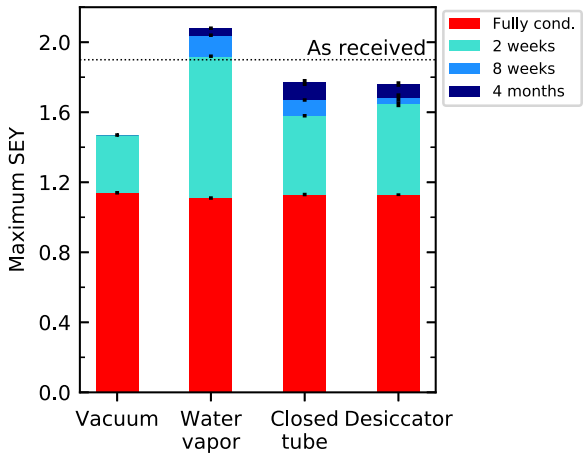

FIG. 7. Evolution of the maximum SEY of samples stored in different atmospheres after full conditioning. The vacuum storage was performed for only 2 weeks.

the accelerator, samples were partially conditioned down to different maximum SEY by stopping the conditioning at different doses. These samples were then immediately stored in a desiccator. Their maximum SEY was measured after 2 weeks, 8 weeks, and 4 months of storage. Results are shown in Fig. 6 as a function of the SEY obtained by partial conditioning.

After 2 weeks of storage, a clear trend is observed for samples conditioned to a maximum SEY between 1.2 and 1.7: the higher the maximum SEY after conditioning, the higher the maximum SEY after 2 weeks of storage. Instead, all samples with an initial maximum SEY of about 1.12 (fully conditioned) lie in a $\delta_{\max}$ range of 1.58 ± 0.05. As it is visible from Fig. 6, a value of $\delta_{\max}$ in the range 1.58 ± 0.05 after 2 weeks of storage could come from any sample with a maximum SEY between 1.1 and 1.45 after conditioning. The contrast is thus actually lost for any conditioning below $\delta_{\max} = 1.45$. Furthermore, the spread after storage in between the fully conditioned samples (SEY after conditioning around 1.12) is larger than for the partially conditioned samples. This observation is coherent with Fig. 1, where the two fully conditioned samples exhibit different SEY after weeks of storage. For the set of fully conditioned samples in Fig. 6, it is worth mentioning that the SEY after full conditioning is independent from their carbon amount on the surface after irradiation. On the same line, the SEY increase observed for these samples during storage does not correlate with their carbon amount after irradiation, with their carbon amount increase, nor with their hydroxide amount increase during storage, separately. The observed SEY spread after storage is thus likely due to a combination of these different quantities. More data points would be required to disentangle the role of these different contributions. After 8 weeks of storage, the SEY globally increased, and the limit between distinguishable and nondistinguishable samples is now at $\delta_{\max} = 1.55$ after conditioning. After 4 months of storage, all samples lie within a maximum SEY window of 0.15 width, and their distribution seems random in this range, regardless their maximum SEY after conditioning.

D. Influence of the storage atmosphere

The impact of the storage conditions on the deconditioning kinetics was studied by storing samples in different atmospheres after a full conditioning process, in analogy to the case presented in Secs. III. A and III. B for the desiccator storage. The evolution of the maximum SEY of these samples was followed for 2 weeks, 8 weeks, and 4 months of storage (except for vacuum storage, performed for only 2 weeks for logistics reason) and is reported in Fig. 7. Figure 8 displays the maximum SEY of these samples plotted as a function of their $I_{Cu(OH)_2}/I_{Cu,Cu_2O}$ ratio and as a function of their carbon concentration. For the storage in a desiccator, a single sample was selected, close to the average SEY value of all the fully conditioned samples presented in Fig. 6.

It clearly appears that the increase of SEY occurring after extraction of the sample from the UHV analysis setup can be either slowed down or dramatically accelerated by the storage medium. The storage in a stainless-steel tube allows for an equivalent preservation of the SEY to the storage in a desiccator. Besides, these two samples exhibit similar evolution of the $Cu(OH)_2$ and carbon amounts over storage time [Fig. 8, circles and squares]. The sample stored in saturated vapor pressure of water undergoes the fastest SEY increase. After only 2 weeks in a humid atmosphere, the SEY is found at the level of the as received state. In parallel, a rapid growth of hydroxide is observed on the surface [Fig. 8(a), triangles]: after only 2 weeks in a humid atmosphere, the hydroxide amount of this sample is higher than that of the samples stored in the stainless-steel tube or

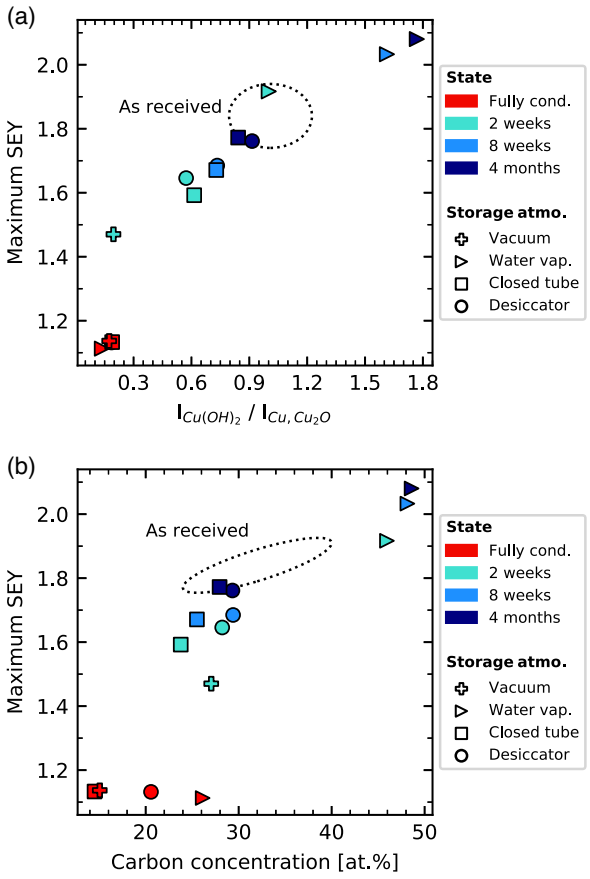

FIG. 8. Maximum SEY as a function of (a) the $I_{Cu(OH)_2}/I_{Cu,Cu_2O}$ ratio and (b) the carbon concentration, for the fully conditioned state and after 2 weeks, 8 weeks, and 4 months storage in different atmospheres. The ellipses indicate the regions corresponding to the as received state of the different samples.

in the desiccator for 4 months. This sample also undergoes a larger carbon uptake than other samples, which is mostly completed after 2 weeks of storage. On the contrary, storage in vacuum efficiently limits the SEY increase. The observed SEY increase of 0.3 in 2 weeks can be easily ascribed to the 1 h air exposure which was required for the transfer of this sample from the UHV analysis setup to the storage chamber. Indeed, this increase is similar to the one observed for 1 h dry air exposure in Fig. 1. In parallel, the hydroxide growth on the surface of this sample is negligible; only carbon contamination is observed [Fig. 8, crosses].

IV. DISCUSSION

In real cases, i.e., the analysis of surfaces of components extracted from accelerators, a comparison between "as extracted" and "as received" states is not always possible. Indeed, the surface state before accelerator operation is often not precisely characterized and may present some scattering along the beam pipes. Therefore, the assessment of beam-induced modifications of the surfaces of accelerator-extracted components is often only based on the as extracted characterization, which may limit the accessible information. However, in the present laboratory case, the as received state of the samples was systematically characterized. This allows carrying out a complete analysis of the deconditioning mechanisms and memory effect.

SEY reduction, surface cleaning through conversion of $Cu(OH)_2$, and ESD of hydrocarbons, as well as carbon graphitization, were observed during conditioning of an air-exposed copper surface. The reverse processes are thus expected to occur when a conditioned surface is exposed again to air. Indeed, during storage in a desiccator, an SEY increase is observed for all samples, regardless of their SEY after conditioning. For a fully conditioned sample, a fast loss of conditioning state, i.e., SEY increase, occurs immediately at air exposure. The SEY keeps then increasing over months, more and more slowly. A corresponding increase of the $Cu(OH)_2$ component is observed, together with an increase of the atomic carbon concentration, as expected during air exposure of copper [37]. Both hydroxide and airborne adsorbed hydrocarbons are known to increase the yield of a clean surface [28,32,33]. The observed SEY increase during storage can thus be ascribed to the buildup of these species onto the conditioned surface. As a confirmation, the sample stored in a humid atmosphere undergoes the strongest recontamination by hydroxide and carbon (the sample was not wrapped in aluminum foil during storage) and also the highest SEY increase.

For the desiccator case, carbon recontamination is immediate (timescale of minutes) at air exposure, while the buildup of hydroxide requires more time. It is also observed that, while carbon uptake almost saturates after 2 weeks of storage in a humid atmosphere, the hydroxide keeps building up on the surface of this sample for the following weeks. Such a difference of timescale can be due to the different mechanisms behind these recontaminations. While carbon adsorption is immediate at air exposure due to the high surface energy of the clean conditioned surface, hydroxide growth involves the dissociative adsorption of water followed by the reaction of copper ions with the adsorbed hydroxyl groups [38–41]. The mechanism of carbon increase by adsorption corresponds well to the general shape of the curve in Fig. 4 for the carbon concentration, which flattens and saturates when the surface is completely covered and the sticking coefficient decreases. It is shown, by storage in different atmospheres, that the kinetics of the two effects can be further influenced by the storage conditions and relative abundance of water and hydrocarbons.

It is worth remarking that in spite of the graphitization, i.e., modification of the surface airborne hydrocarbons to graphite during conditioning, there is no strong passivation effect on the surface. For the case of the adsorption of hydrocarbons, this is explained by the fact that even if the

surface energy of graphite (54–127 mJ/m^2 [42,43]) or graphene [42] is lower than that of metals and oxides (100–1000 mJ/m^2 [43]), it remains higher than that of most hydrocarbons (about 25 mJ/m^2 for alkanes [44]), and, therefore, a full hydrocarbon coverage of the surface is thermodynamically favored. Again, this is in agreement with the flattening of the carbon concentration curve in Fig. 4 for long storage times, since the resulting sticking probability of hydrocarbons on a hydrocarbon layer is expected to be weaker than for hydrocarbons on a clean surface. For the formation of the hydroxide, the graphitic layer is not sufficient to protect from a further reaction either because it is not fully covering the surface or because it is not an effective barrier to chemical reactions. In this sense, the role of graphene layers on top of copper is still unclear [45], and so is the effect of the graphitic layer formed during irradiation. A study of hydroxide formation as a function of the amount of carbon could better disentangle the two arguments.

According to the above-mentioned mechanisms of deconditioning, storage of the conditioned surfaces in a clean and dry atmosphere is clearly ideal. Indeed, excellent preservation of the SEY was obtained while storing a conditioned sample in vacuum after a 1 h transfer in air from the UHV analysis setup to the storage chamber. Such a low SEY increase relies, in particular, on the mitigation of hydroxide buildup and is due only to carbon recontamination during the transfer. Unfortunately, the data in Fig. 4 display an increase of the SEY during dry air exposure, which is almost linear on a logarithmic timescale. This reflects a very fast increase occurring at the very beginning of the air exposure, and the further deterioration of the surface properties proceeds more slowly.

As discussed above, this fast initial deterioration is ascribed to the hydrocarbon adsorption and is almost unavoidable for practical application, where components must be extracted from an accelerator. Indeed, in such cases, the exposure to air before the analyses can last for weeks [27]. In addition, collecting samples from a vacuum component of an accelerator may involve steps like drilling, cutting, etc., which may further degrade their surface state.

This has a consequence on the possibility to detect a contrast between more or less conditioned areas of the surface. For samples conditioned to a maximum SEY below 1.45, the maximum SEY after 2 weeks in a desiccator lies in a range of 0.1 centered around 1.58. The contrasts existing between these samples at the end of the conditioning are thus erased by the 2 weeks of storage. Such an effect results from a higher SEY increase for the most conditioned samples. Considering the proposed deconditioning mechanisms, a hypothesis for this behavior is an increased surface reactivity of the most conditioned samples driven by their stronger surface modification during conditioning. For an SEY after conditioning above 1.45, the contrasts are still present after 2 weeks. Therefore, an estimate of the *in situ* SEY could be deduced from the SEY after 2 weeks of venting.

The above-mentioned findings have various practical consequences. First, in view of saving conditioning time at the resume of the operation after venting, the vacuum system should be kept in a dry atmosphere, exempt from hydrocarbons. In this context, it is worth mentioning that storage in a desiccator, which is clearly unpractical for large components, is equivalent to a vacuum system closed on itself after air venting (Figs. 7 and 8, closed tube). On the same line, the venting should be performed with a dry gas, e.g., nitrogen-oxygen mixture, and exposure to the ambient atmosphere should be limited at most.

Second, for the surface analysis of components extracted from their operational environment, stopping the deconditioning in a controlled way after extraction is of particular importance to ensure comparability of the different surfaces, if the analyses spread over long timescales.

Third, the logarithmic behavior implies that a loss of the *in situ* conditioning state irremediably happens if air exposure of the surface—even of short duration—is required. The air exposure erases the *in situ* conditioning contrasts, and within 2 weeks of dry air exposure it is impossible to distinguish between surfaces having an advanced conditioning state, i.e., with an SEY in a crucial region spanning, for instance, just above and below the threshold for electron cloud buildup in a machine like the LHC [46]. Therefore, if such contrasts have to be investigated, the analyses should be performed after the shortest possible venting time, and the limit of the accessible information for the particular storage time and conditions has to be taken into account while interpreting the results.

V. CONCLUSIONS

The kinetics and mechanisms of deconditioning were studied for a copper surface stored in a desiccator after full conditioning by electron irradiation. An immediate SEY increase is observed at venting, driven by a recontamination of the surface by carbon adsorption and hydroxide growth. It is demonstrated that, during storage in a desiccator, the SEY contrasts present after conditioning between different samples tend to disappear, due to a faster SEY increase for the most conditioned samples. Therefore, if vacuum components have to be exposed to air before their surface analysis, some *in situ* SEY contrasts may irreversibly be lost, limiting the level of information accessible with such analyses. However, the memory effect of the conditioning is still clearly present after 4 months of dry air exposure.

It is then demonstrated that the storage conditions significantly impact the deconditioning kinetics. While a conditioned sample recovers the as received SEY value after only 2 weeks of storage in a humid atmosphere, vacuum is found to efficiently hinder the SEY increase of the conditioned surface. However, intermediate storage

options, like closing the vented beam pipe on itself, allow for a reasonable preservation of the conditioning state while being more easily implemented than vacuum storage. In this case, the venting atmosphere is of particular importance, and venting should be performed with a dry and clean gas.

ACKNOWLEDGMENTS

The authors thank M. Himmerlich for the useful discussions and critical reading of this manuscript.

[1] W. Fischer, M. Blaskiewicz, J. M. Brennan, H. Huang, H. C. Hseuh, V. Ptitsyn, T. Roser, P. Thieberger, D. Trbojevic, J. Wei, S. Y. Zhang, and U. Iriso, Electron cloud observations and cures in the Relativistic Heavy Ion Collider, Phys. Rev. Accel. Beams **11**, 041002 (2008).

[2] H. Fukuma, Electron cloud effects in KEKB, in *Proceedings of Mini Workshop on Electron Cloud Simulations for Proton and Positron Beams—ECLOUD'02, Geneva, Switzerland, 2002* (CERN, Geneva, 2002), p. 1.

[3] H. Fukuma, K. Ohmi, Y. Suetsugu, and M. Tobiyama, Electron cloud at SuperKEKB, in *Proceedings of ICFA Advanced Beam Dynamics Workshop on High Luminosity Circular e^+e^- Colliders (eeFACT'16), Daresbury, UK, 2016* (JACoW, Geneva, Switzerland, 2017), p. 125.

[4] G. Rumolo, H. Bartosik, E. Belli, P. Dijkstal, G. Iadarola, K. Li, L. Mether, A. Romano, M. Schenk, and F. Zimmermann, Electron cloud effects at the LHC and LHC injectors, in *Proceedings of the 8th International Particle Accelerator Conference: IPAC 2017, Copenhagen, Denmark, 2017* (JACoW, Geneva, Switzerland, 2017), p. 30.

[5] C. Y. Vallgren, G. Arduini, J. Bauche, S. Calatroni, P. Chiggiato, K. Cornelis, P. C. Pinto, B. Henrist, E. Métral, H. Neupert, G. Rumolo, E. Shaposhnikova, and M. Taborelli, Amorphous carbon coatings for the mitigation of electron cloud in the CERN Super Proton Synchrotron, Phys. Rev. Accel. Beams **14**, 071001 (2011).

[6] P. Chiggiato and P. C. Pinto, Ti-Zr-V non-evaporable getter films: From development to large scale production for the Large Hadron Collider, Thin Solid Films **515**, 382 (2006).

[7] S. Calatroni, E. G.-T. Valdivieso, H. Neupert, V. Nistor, A. T. P. Fontenla, M. Taborelli, P. Chiggiato, O. Malyshev, R. Valizadeh, S. Wackerow, S. A. Zolotovskaya, W. A. Gillespie, and A. Abdolvand, First accelerator test of vacuum components with laser-engineered surfaces for electron-cloud mitigation, Phys. Rev. Accel. Beams **20**, 113201 (2017).

[8] R. Valizadeh, O. B. Malyshev, S. Wang, S. A. Zolotovskaya, W. A. Gillespie, and A. Abdolvand, Low secondary electron yield engineered surface for electron cloud mitigation, Appl. Phys. Lett. **105**, 231605 (2014).

[9] H. Fukuma, J. Flanagan, K. Hosoyama, T. Ieiri, T. Kawamoto, T. Kubo, M. Suetake, S. Uno, S. S. Win, and M. Yoshioka, Status of solenoid system to suppress the electron cloud effects at the KEKB, AIP Conf. Proc. **642**, 357 (2002).

[10] Y. Suetsugu, H. Fukuma, L. Wang, M. Pivi, A. Morishige, Y. Suzuki, M. Tsukamoto, and M. Tsuchiya, Demonstration of electron clearing effect by means of a clearing electrode in high-intensity positron ring, Nucl. Instruments Methods Phys. Res., Sect. A **598**, 372 (2009).

[11] O. Brüning, P. Collier, P. Lebrun, S. Myers, R. Ostojic, J. Poole, and P. Proudlock, LHC design report, CERN, Geneva, 2004.

[12] Y. Suetsugu, K. Kanazawa, K. Shibata, T. Ishibashi, H. Hisamatsu, M. Shirai, and S. Terui, Design and construction of the SuperKEKB vacuum system, J. Vac. Sci. Technol. A **30**, 031602 (2012).

[13] Y. Suetsugu, K. Shibata, T. Ishibashi, H. Fukuma, M. Tobiyama, J. Flanagan, E. Mulyani, M. Shirai, S. Terui, K. Kanazawa, and H. Hisamatsu, Achievements and problems in the first commissioning of SuperKEKB vacuum system, J. Vac. Sci. Technol. A **35**, 03E103 (2017).

[14] C. Scheuerlein, M. Taborelli, N. Hilleret, A. Brown, and M. A. Baker, An AES study of the room temperature conditioning of technological metal surfaces by electron irradiation, Appl. Surf. Sci. **202**, 57 (2002).

[15] M. T. F. Pivi, G. Collet, F. King, R. E. Kirby, T. Markiewicz, T. O. Raubenheimer, J. Seeman, and F. Le Pimpec, Experimental observations of in situ secondary electron yield reduction in the PEP-II particle accelerator beam line, Nucl. Instruments Methods Phys. Res., Sect. A **621**, 47 (2010).

[16] B. Henrist, N. Hilleret, C. Scheuerlein, M. Taborelli, and G. Vorlaufer, The variation of the secondary electron yield and of the desorption yield of copper under electron bombardment: origin and impact on the conditioning of the LHC, in *Proceedings of the 8th European Particle Accelerator Conference, Paris, 2002* (EPS-IGA and CERN, Geneva, 2002), p. 2553.

[17] M. Nishiwaki and S. Kato, Electron stimulated gas desorption from copper material and its surface analysis, Appl. Surf. Sci. **169–170**, 700 (2001).

[18] V. Petit, M. Taborelli, H. Neupert, P. Chiggiato, and M. Belhaj, Role of the different chemical components in the conditioning process of air exposed copper surfaces, Phys. Rev. Accel. Beams **22**, 083101 (2019).

[19] R. Larciprete, D. R. Grosso, M. Commisso, R. Flammini, and R. Cimino, Secondary electron yield of Cu technical surfaces: Dependence on electron irradiation, Phys. Rev. Accel. Beams **16**, 011002 (2013).

[20] R. Cimino, M. Commisso, D. R. Grosso, T. Demma, V. Baglin, R. Flammini, and R. Larciprete, Nature of the Decrease of the Secondary-Electron Yield by Electron Bombardment and Its Energy Dependence, Phys. Rev. Lett. **109**, 064801 (2012).

[21] M. Nishiwaki and S. Kato, Graphitization of inner surface of copper beam duct of KEKB positron ring, Vacuum **84**, 743 (2009).

[22] C. Scheuerlein and M. Taborelli, Electron stimulated carbon adsorption in ultrahigh vacuum monitored by Auger electron spectroscopy, J. Vac. Sci. Technol. A **20**, 93 (2002).

[23] S. Kato and M. Nishiwaki, In-situ SEY measurements at KEKB positron ring and comparison with laboratory experiments, in *Proceedings of the International Workshop on Electron-Cloud Effects, ECLOUD'07, Daegu,*

Korea, 2007 [High Energy Accelerator Research Organization (KEK), Tsukuba, (2007)], p. 72.

[24] W. Hartung, J. Conway, C. Dennett, S. Greenwald, J.-S. Kim, Y. Li, T. Moore, and V. Omanovic, Measurements of secondary electron yield of metal surfaces and films with exposure to a realistic accelerator environment, in *Proceedings of the 4th International Particle Accelerator Conference, IPAC-2013, Shanghai, China, 2013* (JACoW, Geneva, Switzerland, 2013), p. 3493.

[25] V. Baglin, I. R. Collins, O. Gröbner, C. Grünhagel, B. Henrist, N. Hilleret, and B. Jenninger, Measurements at EPA of vacuum and electron-cloud related effects, in *Proceedings of the 11th Workshop of the LHC, Chamonix XI, Chamonix, France, 2001* (CERN, Geneva, 2001), p. 141.

[26] J. M. Jimenez, G. Arduini, P. Collier, G. Ferioli, B. Henrist, N. Hilleret, L. Jensen, K. Weiss, and F. Zimmermann, Electron cloud with LHC-type beams in the SPS: a review of three years of measurements, in *Proceedings of the Mini Workshop on Electron Cloud Simulations for Proton And Positron Beams, ECLOUD'02, Geneva, Switzerland, 2002* (CERN, Geneva, 2002), p. 17.

[27] V. Petit, H. Neupert, E. G.-T. Valdivieso, M. Taborelli, and M. Belhaj, Surface characterization of vacuum components extracted from LHC dipole magnet, in *Proceedings of the 6th Electron-Cloud Workshop ECLOUD'18, La Biodola, Italy, 2018* (to be published).

[28] I. Bojko, N. Hilleret, and C. Scheuerlein, Influence of air exposures and thermal treatments on the secondary electron yield of copper, J. Vac. Sci. Technol. A **18**, 972 (2000).

[29] C. Scheuerlein and M. Taborelli, The assessment of metal surface cleanliness by XPS, Appl. Surf. Sci. **252**, 4279 (2006).

[30] N. S. Mclntyre and M. G. Cook, X-ray photoelectron studies on some oxides and hydroxides of cobalt, nickel, and copper, Anal. Chem. **47**, 2208 (1975).

[31] T. Robert, M. Bartel, and G. Offergeld, Characterization of oxygen species adsorbed on copper and nickel oxides by x-ray photoelectron spectroscopy, Surf. Sci. **33**, 123 (1972).

[32] N. Hilleret, C. Scheuerlein, and M. Taborelli, The secondary-electron yield of air-exposed metal surfaces, Appl. Phys. A **76**, 1085 (2003).

[33] J. Halbritter, On changes of secondary emission by resonant tunneling via adsorbates, J. Phys. (Paris), Colloq. **45**, C2-315 (1984).

[34] J. Díaz, G. Paolicelli, S. Ferrer, and F. Comin, Separation of the sp^3 and sp^2 components in the C1s photoemission spectra of amorphous carbon films, Phys. Rev. B **54**, 8064 (1996).

[35] J. Kim, S. K. Baek, K. S. Kim, Y. J. Chang, and E. J. Choi, Long-term stability study of graphene-passivated black phosphorus under air exposure, Curr. Appl. Phys. **16**, 165 (2016).

[36] H. Y. Nan, Z. H. Ni, J. Wang, Z. Zafar, Z. X. Shi, and Y. Y. Wang, The thermal stability of graphene in air investigated by Raman spectroscopy, J. Raman Spectrosc. **44**, 1018 (2013).

[37] S. K. Chawla, B. I. Rickett, N. Sankarraman, and J. H. Payer, An x-ray photoelectron spectroscopic investigation of the air-formed film on copper, Corros. Sci. **33**, 1617 (1992).

[38] I. Platzman, R. Brener, H. Haick, and R. Tannenbaum, Oxidation of polycrystalline copper thin films at ambient conditions, J. Phys. Chem. C **112**, 1101 (2008).

[39] Y. P. Timalsina, M. Washington, G. C. Wang, and T. M. Lu, Slow oxidation kinetics in an epitaxial copper (100) film, Appl. Surf. Sci. **363**, 209 (2016).

[40] S. Yamamoto, K. Andersson, H. Bluhm, G. Ketteler, D. E. Starr, T. Schiros, H. Ogasawara, L. G. M. Pettersson, M. Salmeron, and A. Nilsson, Hydroxyl-induced wetting of metals by water at near-ambient conditions, J. Phys. Chem. C **111**, 7848 (2007).

[41] Z. J. Zuo, J. Li, P. De Han, and W. Huang, XPS and DFT studies on the autoxidation process of Cu sheet at room temperature, J. Phys. Chem. C **118**, 20332 (2014).

[42] S. Wang, Y. Zhang, N. Abidi, and L. Cabrales, Wettability and surface free energy of graphene films, Langmuir **25**, 11078 (2009).

[43] Y. I. Tarasevich, Surface energy of oxides and silicates, Theor. Exp. Chem. **42**, 145 (2006).

[44] A. Romero-Martínez and A. Trejo, Surface tension of pure hydrocarbons, Int. J. Thermophys. **19**, 1605 (1998).

[45] F. Zhou, Z. Li, G. J. Shenoy, L. Li, and H. Liu, Enhanced room-temperature corrosion of copper in the presence of graphene, ACS Nano **7**, 6939 (2013).

[46] G. Skripka and G. Iadarola, Beam-induced heat loads on the beam screens of the HL-LHC arcs, Report No. CERN-ACC-NOTE-2019-0041, Geneva, Switzerland.